PPLN-Based Optical Parametric Amplification for Wideband WDM Transmission

Shimpei Shimizu, *Member, IEEE*, Takayuki Kobayashi, *Member, IEEE*, Takushi Kazama, Takeshi Umeki, *Member, IEEE*, Masanori Nakamura, *Member, IEEE*, Koji Enbutsu, Takahiro Kashiwazaki, Ryoichi Kasahara, Kei Watanabe, and Yutaka Miyamoto, *Member, IEEE*

(Invited Paper)

***Abstract*—The optical parametric amplifier (OPA) has attractive features for optical communications, such as a wideband, high gain, and fast transient response. In addition, by using idler light, which is phase-conjugated light generated in the amplification process, various kinds of optical signal processing, such as fiber-nonlinearity mitigation, wavelength conversion, and phase-sensitive amplification, can be performed. A periodically poled $LiNbO_3$ (PPLN) waveguide is an $\chi^{(2)}$-based optical parametric amplification medium, and it makes both wideband and high-gain amplification possible. We developed a 4-port PPLN module that can combine signal light and pump light into a PPLN waveguide with low loss. In this paper, we overview the applications of OPA to WDM optical fiber transmission and explain the configurations of an OPA using 4-port PPLN modules. As applications of our PPLN-based OPA, we introduce the demonstration of wideband inline amplification exceeding 5 THz. Furthermore, we demonstrate inter-band wavelength conversion between C- and S-bands using PPLN waveguides developed for multi-band optical transmission applications.**

***Index Terms*—Nonlinear optics, optical amplifiers, optical fiber communication.**

I. INTRODUCTION

OPTICAL Transport networks using wavelength-division multiplexing (WDM) and digital coherent technology have been widely deployed. For increasing the transmission throughput to meet the demand for high-speed communications, spectrally efficient modulation formats, such as higher-order quadrature-amplitude modulation (QAM), and transmission bandwidth extension are effective. Recently, using a probabilistically shaped (PS-) 64QAM signal, 1-Tbps/ch. full C-band WDM transmission was demonstrated over 800 km [1]. Spectrally efficient signals require a high signal-to-noise ratio (SNR) according to the Shannon theorem. In the region linear with respect to the input power, the SNR of the received signal is improved as the optical SNR (OSNR) increases given that the SNR of the electrical signal provided to the optical modulator is sufficient. However, excess fiber-input power to increase OSNR brings strong fiber nonlinearity, which causes signal distortion induced by self-phase modulation (SPM), cross-phase modulation (XPM), and four-wave mixing (FWM). In such nonlinear region, the OSNR improves as the input power increases, but the SNR of the received signal deteriorates. Thus, fiber-input power is limited by fiber nonlinearity. In addition, it is well-known that phase-insensitive amplifiers (PIAs) such as erbium-doped fiber amplifiers (EDFAs) output excessive amplified spontaneous emission (ASE) noise corresponding to a noise figure (NF) of >3 dB. Therefore, transmission bandwidth extension and optical signal-processing such as fiber-nonlinearity mitigation for improving SNR are important techniques for further enhancing the transmission throughput in optical fiber communications.

In deployed WDM transmission systems, EDFAs, which typically have a 4-THz amplification bandwidth in the C- or L-bands, are widely used as inline optical repeaters. The conventional systems have been designed for this EDFA band. To extend the optical transmission bandwidth and realize multi-band optical networks using S-, C-, and L-bands, various wideband optical repeater configurations have been proposed such as a hybrid configuration of Raman amplification and EDFAs [2], [3], all-Raman amplification [4], [5], multiple rare-earth-doped fiber amplifiers with different amplification bands [6], and a semiconductor optical amplifier [7]. The optical parametric amplifier (OPA) is also attracting attention in research as a wideband optical amplifier outperforming the EDFA band. OPAs utilizing nonlinear optical processes have been studied using periodically poled $LiNbO_3$ (PPLN) waveguides as a $\chi^{(2)}$-based medium [8]–[13] or highly nonlinear fibers (HNLFs) as a $\chi^{(3)}$-based medium [14]–[19]. Recently, a highly efficient $\chi^{(3)}$-based OPA using a silicon nitride waveguide was also proposed [20]. The attractive features of the OPA are a wideband [8], [12], [15], [16], high gain [12], [13], [17], and small gain-transient response [18], [19].

Manuscript received September 29, 2021; revised December 20, 2021; accepted January 7, 2022. Date of publication January 13, 2022; date of current version June 1, 2022. *(Corresponding author: Shimpei Shimizu.)*

Shimpei Shimizu, Takayuki Kobayashi, Masanori Nakamura, and Yutaka Miyamoto are with NTT Network Innovation Labs., NTT Corporation, Yokosuka 239-0847, Japan (e-mail: shimpei.shimizu.ge@hco.ntt.co.jp; takayuki.kobayashi.wt@hco.ntt.co.jp; masanori.nakamura.cu@hco.ntt.co.jp; yutaka.miyamoto.fb@hco.ntt.co.jp).

Takushi Kazama, Takeshi Umeki, and Kei Watanabe are with NTT Network Innovation Labs., NTT Corporation, Yokosuka 239-0847, Japan, and also with the NTT Device Technology Laboratories, NTT Corporation, Atsugi 243-0198, Japan (e-mail: takushi.kazama.me@hco.ntt.co.jp; takeshi.umeki.zv@hco.ntt.co.jp; kei.watanabe.hg@hco.ntt.co.jp).

Koji Enbutsu, Takahiro Kashiwazaki, and Ryoichi Kasahara are with NTT Device Technology Laboratories, NTT Corporation, Atsugi 243-0198, Japan (e-mail: koji.enbutsu.cm@hco.ntt.co.jp; takahiro.kashiwazaki.dy@hco.ntt.co.jp; ryoichi.kasahara.fs@hco.ntt.co.jp).

Color versions of one or more figures in this article are available at https://doi.org/10.1109/JLT.2022.3142749.

Digital Object Identifier 10.1109/JLT.2022.3142749

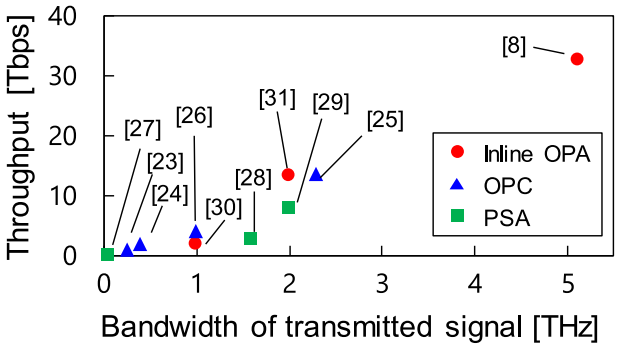

Fig. 1. Representative demonstrations of WDM fiber transmission utilizing OPAs as inline OPA, OPC, and PSA.

An inherent feature of the OPA is that idler light is generated at a wavelength symmetric with respect to the center of the amplification band of the OPA while signal light is amplified. Using idler light, spectral inversion, which is the simultaneous flipping of the signal spectrum, can be performed. Utilizing this function of the OPA, wavelength conversion of signal light can be performed [21]. To achieve multi-band optical transmission, a system configuration using wavelength conversion by OPA has been proposed, and WDM transmission with this configuration using triple bands of the S-, C-, and L-bands was recently demonstrated [22]. Also, idler light is characterized by being a phase-conjugated copy of input signal light. A method of compensating for nonlinear distortion by performing phase conjugation of signal light at a relay node has been studied, namely optical phase conjugation (OPC) [23]–[26]. A phase-sensitive amplifier (PSA) is also one application of optical parametric amplification [27]–[29]. Phase-sensitive amplification is a method of obtaining additional gain by causing coherent superposition between signal light and idler light during the optical parametric amplification process. With this additional coherent gain, the PSA can realize ultra-low-noise optical amplification that is below the 3-dB NF limit of PIAs. As described above, by using idler light, the OPA can perform all-optical signal processing that improves the SNR outperforming conventional limits by compensating for nonlinear distortion and suppressing ASE noise.

Many researchers have demonstrated WDM transmission using the OPA. Fig. 1 shows representative demonstrations of WDM transmission utilizing the OPA as an inline amplifier, OPC, and PSA. The horizontal axis is the bandwidth of the transmitted WDM signal, and the vertical axis is the throughput claimed in the papers. An OPA with an over-100-nm wide-amplification bandwidth has been reported many times using measurements sweeping CW light [12], [16], [17]. However, there have been no demonstrations of WDM fiber transmission with simultaneous wideband optical parametric amplification outperforming the EDFA band. Also, the symbol rate and the modulation format of the transmitted signals were the standard ones, and thus, only a small total throughput was shown in comparison with state-of-the-art WDM transmission experiments. Recently, we demonstrated inline-amplified transmission using PPLN-based OPA-only repeaters with an over-5-THz WDM signal [8]. Each channel in the WDM signal was modulated with 120-Gbaud PS-36QAM in advanced formats, and a 32.8-Tbps total throughput was achieved. In [8], only one side of the amplification band of the OPA was used, so it was shown that 10-THz-class inline amplification using an PPLN-based OPA was feasible.

This paper overviews research progress made on the OPA for WDM optical fiber transmission and describes the configurations and applications of our PPLN-based OPA. In Section II, three applications of OPA for optical communications, as inline amplifiers, spectral invertors, and PSAs, are explained. In Section III, the configuration of an OPA using our 4-port PPLN module and efforts to make OPAs polarization-independent are described. In Section IV, we describe the first demonstration of wideband inline-amplified transmission over 5 THz using OPA-only repeaters [8]. In Section V, we describe inter-band wavelength conversion using a PPLN-based OPA for multi-band optical networks. We fabricated PPLN modules with a center wavelength of the amplification bandwidth between C- and S-bands and demonstrate simultaneous wavelength conversion between the C- and S-bands.

II. Applications of Optical Parametric Amplification for WDM Transmission

This section describes three applications of the OPA for optical communications. Fig. 2 shows their configurations. The same configurations are available for both fiber-based OPAs (FOPAs) and PPLN-based OPAs. Recent research progress on WDM transmission is overviewed.

A. *Wideband Inline Amplifier*

Fig. 2(a) shows the configuration of an inline OPA operated as a PIA. One of the features of optical parametric amplification is a wideband outperforming typical EDFAs. The amplification bandwidth of the OPA depends on the phase-matching characteristics in a nonlinear optical medium. To widen the phase-matching bandwidth, an FOPA uses an optical fiber in which the zero-dispersion wavelength is shifted and the dispersion slope is flattened. To obtain sufficient amplification gain, light propagation in an HNLF of a few hundred meters is generally required. Therefore, fluctuations in the dispersion and polarization states of the amplified light along with fiber propagation are also important. Recently, a wideband FOPA using a polarization-maintaining HNLF with little fluctuation in the zero-dispersion wavelength has been demonstrated with a bandwidth of over 170-nm bandwidth and a gain of over 10 dB [17]. However, FOPAs have some difficulties for wideband WDM signal amplification. In particular, the influence of high-power pump light arranged in the same band as the signal is significant. The high-power pump causes stimulated Brillouin scattering (SBS) and ASE noise around the pump [14], [32]. Therefore, the input-pump power is limited, and a guard band is required around the wavelength of the pump light. Because the output power of OPAs is restricted by the pump power, it is considered that simultaneous amplification of a wideband WDM signal with sufficient gain and power per channel become difficult. To avoid SBS, a pump dithering technique is often used [33]. Moreover, unnecessary FWM,

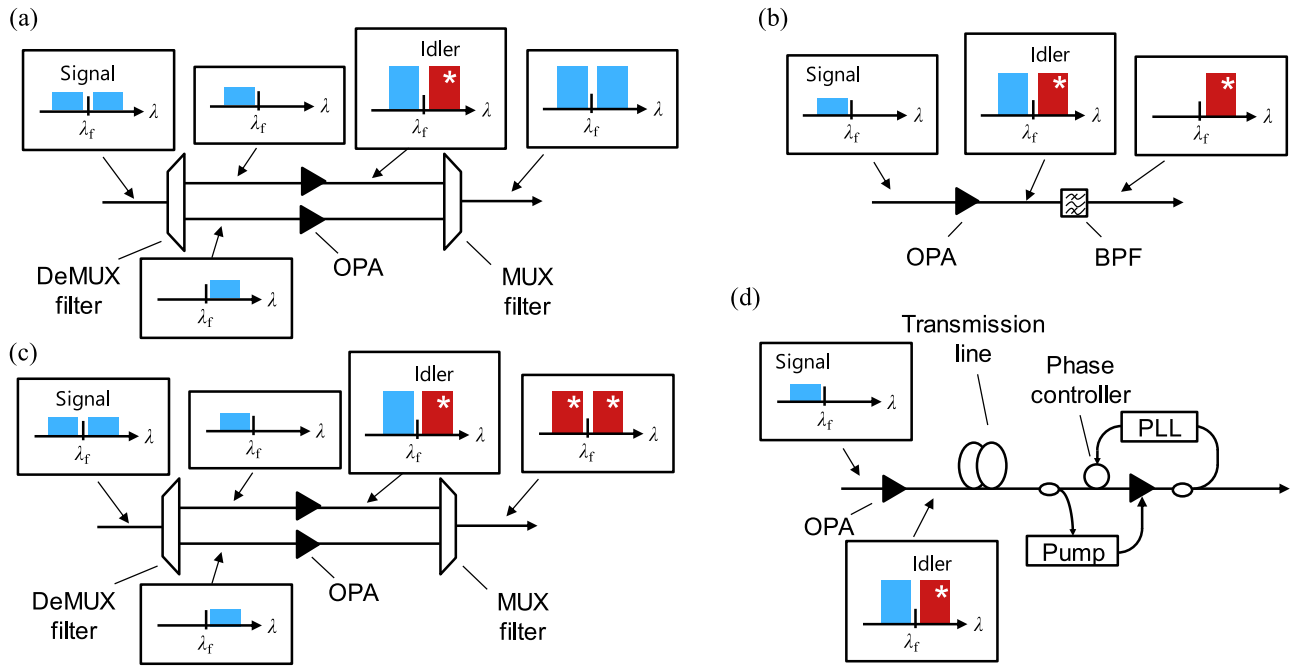

Fig. 2. Applications of OPA for optical communication and their configurations. (a) Inline amplification with full-band configuration. (b) Wavelength conversion. (c) Optical phase conjugation with CSI configuration. (d) Phase-sensitive amplification. λ_f is center wavelength of amplification band.

which induces parametric cross-talk (PXT), occurs due to the nonlinear interaction among WDM channels and restricts the number and power of WDM channels [32]. A fiber design for suppressing the unwanted FWM has been studied [34]. Recently, a silicon nitride waveguide has attracted research attention as a $\chi^{(3)}$-based medium with a high amplification efficiency, high integration, and resistance to unwanted nonlinear effects. An efficient OPA with a precisely dispersion-managed long silicon nitride waveguide has been demonstrated [20]. Although the achieved gain is ~10 dB at present, it has the potential for high gain operation with a low NF and negligible signal distortion.

A PPLN waveguide has a higher amplification efficiency thanks to the high second-order nonlinearity of $LiNbO_3$, quasi-phase-matching (QPM), and its large light-confining effect along the waveguide. Therefore, a sufficient amplification gain is obtained with a short propagation length of few tens of millimeters. Thus, unwanted nonlinear effects such as SBS and FWM can be suppressed [35]. The capability of the input-pump power is limited by photorefractive damage, which deteriorates the condition of the QPM in accordance with the input power. To overcome this issue, a directly bonded ZnO-doped PPLN ridge waveguide was developed for enhancing the tolerance to the input optical power [36]. There have been various other advances in waveguide fabrication techniques [11], [12]. In [12], a high chip-gain of over 30 dB and wide-amplification bandwidth of over 14 THz were demonstrated. Although the connection between the PPLN waveguide and the optical fiber is also an important issue for optical communication applications, a 4-port PPLN module described in the next section was developed [36]. Such advances have made it possible for PPLN-based OPAs to achieve both a high gain and wideband amplification at the same time.

Optical parametric amplification requires a reserve band for idler light regardless of the amplification media. Therefore, signal light can be allocated in only half the amplification band of a medium. To avoid halving the transmission band, a configuration was developed in which the band is divided into two components and amplified by different OPAs [37]–[39]. Fig. 2(a) shows the full-band configuration. The input WDM signal is divided and combined around λ_f, which is the center wavelength for phase-matching condition, by wavelength MUX/DeMUX filters before and after amplification.

Using FOPA-only repeaters, inline-amplified WDM transmission over 25.2-km spans using 20-ch. 50-GHz-spaced 100-Gbps coherent signals has been reported [30]. However, there are no reports of wideband inline amplification using OPA-only repeaters that exceed the EDFA band. Recently, with a PPLN-based OPA-only repeater, we demonstrated 3×30-km wideband WDM transmission using 41-ch. 120-Gbaud dual-polarized (DP-) PS-36QAM signals over 5 THz [8]. In this demonstration, only one side of the amplification band of the OPA was used, so the potential for over 10-THz inline amplification was shown. In addition, we also demonstrated 16×80-km transmission with a 2-THz signal bandwidth, showing the applicability of OPA to long-haul transmissions with a standard span length and many inline amplifications [31].

B. *Spectral Inversion*

Spectral inversion is performed by extracting the idler light generated in the optical parametric amplification process and using it as new signal light [Fig. 2(b)]. This function can be utilized for wavelength conversion [21]. A multi-band transmission scheme was proposed with inter-band wavelength conversion

using an OPA [22]. The WDM signals of the C-band are converted to the L-band and S-band on the transmitter side, and they are converted back to the C-band on the receiver side. With this scheme, multi-band transmission can be implemented using only conventional C-band transponders. The transmission of 240-ch. 200-Gbps signals over 100 nm within S-, C-, and L-bands using only C-band transponders was demonstrated using FOPAs [22]. Furthermore, for a flexible multi-band network, a configuration in which optical wavelength conversion is performed in optical nodes is also being studied [40]. By once converting all signal bands to the C-band, optical cross-connect across all signal bands can be realized. Thus, inter-band wavelength conversion may play an important role in the construction of multi-band optical networks.

The wavelength-converted signal light is a phase-conjugated copy of the original signal light. Therefore, the spectral inversion via optical parametric amplification is also called as OPC. Using the OPC, the effect of compensating for chromatic dispersion (CD) and nonlinear distortion has been demonstrated [23]–[26]. An OPC is inserted in the relay node. The signal undergoes phase rotation due to CD and nonlinear effects in the span before the OPC. After that, the signal light is phase-conjugated by the OPC in the relay node including the phase rotation. The phase rotation is mitigated by propagation through a span after the OPC because the phase rotations before and after OPC are opposite each other. By mitigating for nonlinear distortion, OPC can relax the fiber-input power limit and improve the SNR of the received signal. Like the inline OPA, the OPC can also utilize a configuration that divides the input signal light into two-band components and converts them independently, namely complementary spectral inversion (CSI) configuration, as shown in Fig. 2(c) [37]–[39].

For complete nonlinear compensation by OPC, the nonlinear phase rotations before and after the OPC must match. Therefore, the symmetry of the power map around the point where the OPC is inserted is important. Distributed Raman amplification (DRA) is also used to realize a symmetric power map. In long-haul transmission with DRA, a 20% enhancement in transmission reach by FOPA-based OPC was demonstrated with a 10-ch. 400-Gbps signals over a 1-THz signal bandwidth [26]. A 3,840-km transmission with an over 0.5-dB improvement in the Q^2-factor was also demonstrated with a 92-ch. 25-GHz-spaced DP-16QAM WDM signal, which had a total net rate of 13.6 Tbps, using PPLN-based OPC [25].

C. Phase-Sensitive Amplifier

Phase-sensitive amplification is performed by superposition between signal and idler light during the optical parametric amplification process. PSAs are classified into a frequency degenerate type (D-PSA) and a non-degenerate type (ND-PSA). In a D-PSA, signal light is arranged at λ_f, and the idler component of signal light is generated by optical parametric amplification at the same wavelength as the signal light. As a result, the one-phase component of noise is suppressed by the superposition of the signal and idler light, and a 0-dB NF limit can be achieved. However, a D-PSA is usually only applicable to single-channel amplification at λ_f and can amplify only one-phase components. An ND-PSA has been developed for achieving the phase-sensitive amplification of a WDM signal and multi-level modulated signals utilizing quadrature phase components [28]. Fig. 2(d) shows a system using the ND-PSA. In the ND-PSA scheme, the idler light is arranged at a different frequency as the signal light and is generated at the transmitter side unlike the D-PSA scheme. Idler light is typically generated by the OPC. It co-propagates with the signal light through a transmission line and is input to the OPA. During the optical parametric amplification process, the idler light is converted to the same frequency as the signal light while undergoing phase conjugation. When the relative phase between the signal, idler, and pump light is properly synchronized, an additional gain of 6 dB, except for the OPA's gain, can be obtained thanks to coherent superposition between the signal and idler light. Thus, an effective NF of -3 dB can be achieved. Note that the NF of the ND-PSA for the total input electrical field including the idler light is 0 dB like the D-PSA. The PSA can also mitigate nonlinear phase noise induced by SPM [41] and XPM [42] thanks to a phase regeneration effect. In practice, we have recorded a 1.0-dB NF using a low-loss pump-combiner-integrated PPLN module [43]. To perform phase-sensitive amplification, it is necessary for the signal, idler, and pump light to be appropriately synchronized in their frequency arrangement and relative phase relationship. Therefore, the frequency of pump light is stabilized using an optical injection locking [44] or optical phase-locking loop (PLL) [45]. To compensate for the phase drift between signal and pump light, a PLL using a phase controller such as a piezo-electric-transducer-based fiber stretcher is utilized. In addition, CD compensation is required before amplification to make the relative phase difference between the signal and idler light uniform in the frequency domain.

So far, some WDM transmission experiments with phase-sensitive amplifications using HNLF and PPLN have been demonstrated. Recently, a multi-span transmission using an FOPA as an inline phase-sensitive amplifier was demonstrated with s single-polarized 10-Gbaud signal up to three channels [27], [46]. Using a polarization-diverse PPLN-based OPA, single inline phase-sensitive amplification of 16-ch. 20-Gbaud DP-16QAM signals over a 1.6-THz signal bandwidth was demonstrated [28]. However, to perform wider-band phase-sensitive amplification, it is necessary to accurately compensate for the CD generated during fiber transmission. To overcome this problem, we proposed a method for accurately estimating and compensating for the residual CD of the transmission link [47]. Recently, using this proposed method, we demonstrated 80-km unrepeated transmission with a 20-ch. 96-Gbaud single-polarized PS-64QAM WDM signal in the 2-THz signal band as the widest bandwidth for simultaneous WDM phase-sensitive amplification [29].

III. Configurations of Optical Parametric Amplifier Using 4-port PPLN Waveguide Module

Fig. 3 shows a 4-port PPLN waveguide module we developed for low-excessive-loss optical parametric amplification [36]. Dichroic filters for the MUX/DeMUX between the signal and

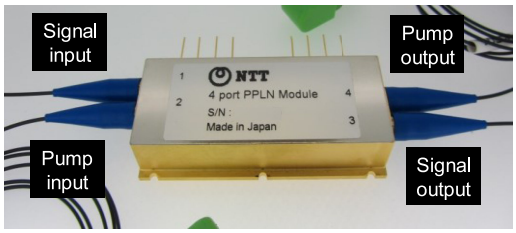

Fig. 3. 4-port PPLN module with size of 66 mm × 24.6 mm × 12 mm.

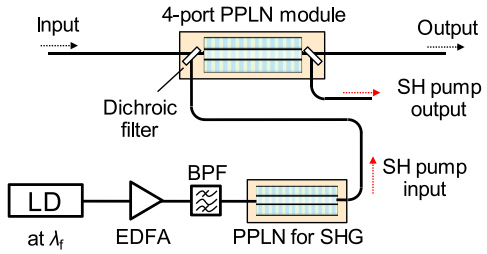

Fig. 4. 2-stage configuration of PPLN-based OPA for suppressing PXT.

pump light and a coupling block to the PPLN waveguide are integrated in the module. The I/O interfaces of the module are simple polarization-maintaining fiber pigtails. This section describes the configuration of an OPA using the 4-port PPLN module.

A. 2-Stage Configuration for Suppressing PXT

In a $\chi^{(2)}$-based OPA, the wavelength of a pump light is half of λ_f. To obtain strong pump light, seed light at λ_f is amplified by EDFA and then converted to the second harmonic (SH) by SH generation (SHG) using a nonlinear medium. A configuration is often utilized in which the conversion of pump light and the optical parametric amplification of signal light are performed in a single nonlinear optical medium [9]–[12]. However, unwanted wavelength conversion in the PPLN waveguide causes PXT. This conversion occurs when the harmonic light generated by the nonlinear interaction among the wavelength components in the signal band acts as detuned pump light. This harmonic light is mostly generated by the strong pump light in the signal band, and the PXT is strongly generated around λ_f. Therefore, a wide guard band is required around λ_f. To suppress the PXT, a 2-stage configuration cascading two PPLNs for SHG and optical parametric amplification was developed [48]. Fig. 4 shows the 2-stage configuration of a PPLN-based OPA using our 4-port PPLN module. Pump light at λ_f is amplified by the EDFA and is then converted to SH light by SHG using a PPLN waveguide different from that for signal amplification. The signal and SH pump light are input to the 4-port PPLN module from different ports, combined by a dichroic filter, and input to the PPLN waveguide for optical parametric amplification. With this configuration, the PXT due to the strong pump light at λ_f is eliminated, and guard-band-less WDM amplification can be realized. Note that the signal cannot be arranged at λ_f, at which the signal and idler light degenerate.

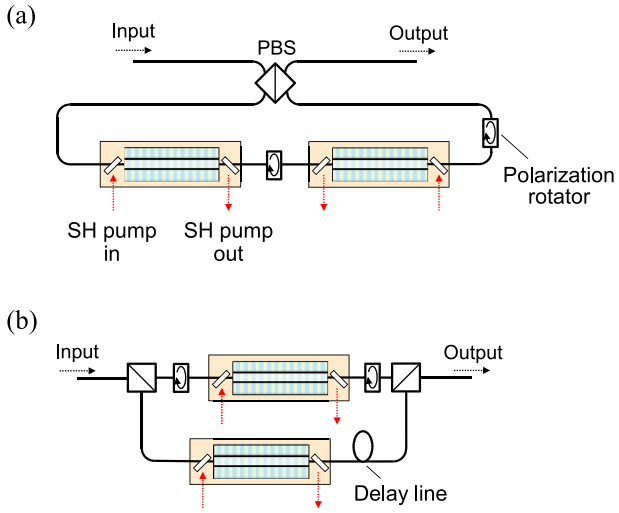

Fig. 5. Polarization-diverse configurations for polarization-insensitive optical parametric amplification. (a) Loop type. (b) Parallel type.

B. Polarization-Diverse Configuration

The nonlinearity in a PPLN waveguide has polarization sensitivity. Also, in HNLF, the optical parametric amplification process depends on the polarization state of the pump light. For polarization-insensitive parametric amplification, polarization-diverse configurations have been studied. For the FOPA, a loop type using a single medium with bi-directional pumping was proposed as the simplest configuration [49]. However, back-propagated light caused by SBS is amplified with counter pump light, causing gain fluctuations and unnecessary interference components [50]. To overcome this issue, a loop type with an independent medium for each orthogonal polarization component has been studied [51]. In this configuration, pump light propagating in opposition does not exist in the medium, and the rotation of the polarization states of signal light between amplification media prevents the amplification of back-propagated light. Thus, the generation of unwanted components can be suppressed. Each polarization component takes amplification in one medium and loss in another. To suppress NF deterioration, it is desirable for signal light to pass through the amplification medium first, but it has been reported that excessive nonlinear distortion occurs when an amplified signal passes through the loss medium [51]. A parallel-type configuration like a Mach-Zehnder interferometer is less susceptible to back-propagated light and does not generate excessive nonlinear optical effects and loss. However, to suppress polarization-mode dispersion (PMD) in the OPA, it is necessary to accurately align the optical path lengths of both arms using an optical delay line [52].

For the PPLN-based OPA, loop-type and parallel-type polarization-diverse configurations with two media have been also studied. Although back-propagated light caused by SBS is sufficiently small, reflected light is generated at the edge of the waveguide. Fig. 5 shows two configurations using 4-port PPLN modules. These configurations are basically the same even when using FOPAs. The 2-stage PPLN-based OPA has fewer unwanted nonlinear effects, and signal light can pass through

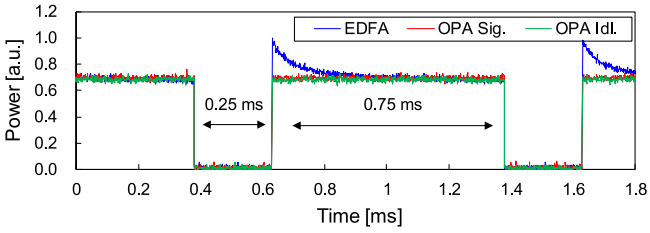

Fig. 6. Comparison of gain transience between EDFA and polarization-diverse PPLN-based OPA.

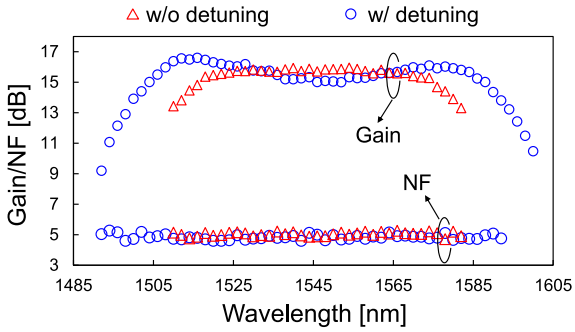

Fig. 7. Gain and NF spectra of our polarization-diverse PPLN-based OPA measured by sweeping CW light with and without detuning of waveguide temperature.

the loss medium without distortion even if it passes through the amplification medium first. Thus, the loop type can be adopted without excessive NF deterioration and signal distortion [53]. However, the transmission loss in a PPLN waveguide acted as a loss medium reduces the total gain. Therefore, in cases where a high gain is required, such as the inline OPA, we have used the parallel type [8], [28]. The loop type, in which the optical path lengths between the two-polarization components match perfectly, is effective for the purpose of optical signal processing that does not require much gain such as OPC.

IV. Fundamental Demonstration of 10-THz Inline PPLN-based Optical Parametric Amplifier

This section describes a fundamental demonstration of inline-amplified transmission using a 10-THz PPLN-based OPA-only repeater [8].

A. Gain Characteristics of PPLN-Based OPA

For polarization-insensitive optical parametric amplification, we used a parallel-type polarization-diverse configuration using four PPLN waveguides with a 1545.32-nm center wavelength for QPM. The length of the PPLN waveguides in the 4-port modules was 45 mm. The core size and length of the PPLN waveguides for the SHG modules were designed for achieving a watt-class SH output power, and those for the 4-port modules were designed for a high amplification efficiency. One of the features of the OPA is that it can track sudden changes in signal power thanks to its fast response time. This characteristic is important for optical transport networks with add/drop/switch for the wavelength channel. We measured the gain transient effect of our PPLN-based OPA to compare it with an EDFA. CW light at 1550.32 nm was input to the polarization-diverse OPA or the EDFA via an optical shutter driven by a 1-kHz rectangular pulse with a 75% duty cycle. After suppressing ASE noise with an optical BPF with a 1-nm bandwidth, output light from the OPA or the EDFA was received by a photodetector, and its time-based waveform was measured by an oscilloscope. The input CW light was -10 dBm, and the gain of the OPA and the EDFA was set to 15 dB. The CW light was distributed to both arms in the polarization-diverse OPA using a polarization controller. Fig. 6 shows the measurement results. For the amplification by the EDFA, it was confirmed that the gain surged upward due to the sudden input of the CW light. In comparison, for the amplification by the OPA, fluctuation in the gain could not be confirmed. Both the signal and idler components had the same characteristic. This is because the EDFA response is on the millisecond scale, while the optical parametric amplification process response is on the femtosecond scale. This result suggests that the OPA is effective in flexible optical networks with frequent channel add/drop.

The amplification bandwidth of optical parametric amplification depends on the phase-matching conditions of the medium. The phase-matching condition can be adjusted to some extent by controlling the temperature of the medium. Under optimal phase-matching conditions, a flat amplification band is obtained around the center wavelength of phase matching. As the temperature is detuned from the optimum conditions, the gain outside the amplification band increases or decreases. The gain near the center wavelength decreases when the outer gain increases, but the amplification bandwidth that achieves the required gain can be extended. The recirculating loop for an inline-amplified transmission experiment described in the next part required an $>$15-dB gain. We performed temperature detuning to obtain a 15-dB gain over a 10-THz bandwidth. Fig. 7 shows the gain and NF spectra of our polarization-diverse PPLN-based OPA before and after temperature detuning as measured by sweeping CW light from 1492 to 1600 nm at a -25-dBm input. The input power of the SH pump light to each 4-port PPLN module was $\sim$1 W, and the input power of the pump light to the PPLN for SHG was $\sim$2 W. The gain and NF were calculated by measuring the input and output spectra of the OPA with an optical spectrum analyzer (OSA) method [54]. By temperature detuning, the bandwidth with an over 15-dB gain was extended from 7.02 THz to 10.54 THz. The NF did not change before and after detuning and was around 5 dB. In the polarization-diverse configuration of the OPA, a polarization dependent gain (PDG) can occur due to the difference in amplification characteristics between the two-amplification media. Fig. 8 shows the output spectrum of each polarization arm, which indicated a PDG spectrum. The input light was unpolarized ASE light from 1545.82 to 1587.25 nm (5.125-THz bandwidth). The input ASE light was generated by combining ASE light from C-band and L-band EDFAs, rectangularly shaped by an optical equalizer (OEQ), and acted as a 125-GHz-spaced 41-channel WDM signal [55]. The amplified spectrum of each arm was measured at a polarization-beam combiner output by disconnecting the other arm. The measured results showed that the two 4-port

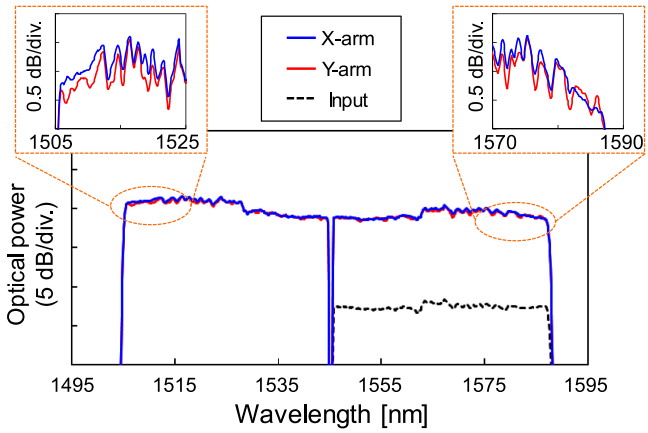

Fig. 8. Spectrum after amplification in each polarization arm of polarization-diverse PPLN-based OPA (0.1-nm resolution). Input light was unpolarized ASE light from 1545.82 to 1587.25 nm.

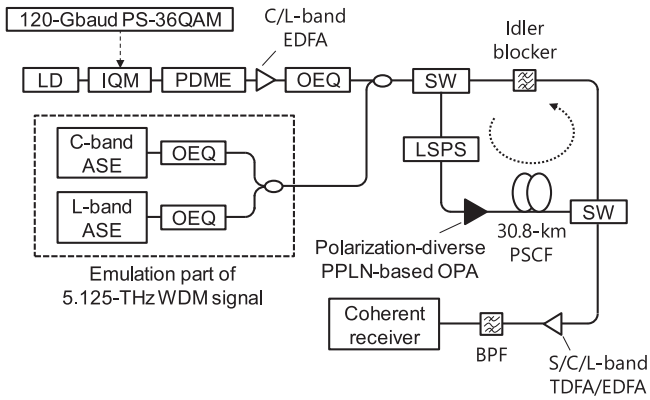

Fig. 9. Experimental setup for wideband inline amplification with PPLN-based OPA. LD: laser diode, IQM: I/Q modulator, PDME: polarization-division multiplexing emulator, SW: optical switch, OEQ: optical equalizer, LSPS: loop-synchronous polarization scrambler, PSCF: pure-silica core fiber, BPF: band-pass filter.

PPLN modules had almost the same amplification characteristics. The PDG of our polarization-diverse OPA was less than 0.5 dB.

B. 41-ch. 120-Gbaud DP-PS-36QAM WDM Transmission Over 3×30-km PSCF Link

Fig. 9 shows the experimental setup for demonstrating inline-amplified transmission using OPA-only repeaters. We utilized a bandwidth loading method using ASE light to emulate the WDM signal [55]. A 125-GHz-spaced 41-channel WDM signal was emulated with the 5.125-THz ASE light used in the previous part. A channel under test (CUT) was modulated at 120 Gbaud using an I/Q modulator (IQM) driven by bandwidth-doubler-based high-speed digital-to-analog converters [56]. The modulation format of the CUT was DP-PS-36QAM with an entropy of 4.435 bits/polarization. Assuming 1.64% pilot-signal insertion, the net data rate was 800 Gbps/ch. with a normalized generalized mutual information (NGMI) threshold of 0.857 [57]. Polarization multiplexing was performed by a polarization-division-multiplexing emulator (PDME) with a 75-ns decorrelation delay. After amplification with either a C- or L-band EDFA according to the CUT's wavelength, the CUT was optically equalized to enhance the high-frequency component [58] and eliminate ASE noise simultaneously. ASE light was rectangularly hollowed out around the wavelength of the CUT with a 125-GHz bandwidth using an OEQ and was then combined with the CUT. A WDM signal consisting of ASE light and the CUT was input to the re-circulating loop. We swept the wavelength of the CUT and measured all 41 channels. The transmission line consisted of a recirculating loop using a 30.8-km G.654.E pure-silica-core fiber (PSCF) with a 125-μm^2 effective area, loop-synchronous polarization scrambler, optical switches, an idler blocker, and the polarization-diverse PPLN-based OPA. The OPA compensated for the losses of the transmission fiber (5.6 dB at 1550 nm), the idler blocker (5.5 dB), and other loop components, over 10.25 THz. The transmission fiber length in the loop was mainly restricted by the insertion loss of the idler blocker, which played the role of MUX/DeMUX filters in the full-band configuration. In the first lap, the OPA played the role of a post-amplifier and wavelength convertor, and the idler light of the launched WDM signal was generated from 1505.55 to 1544.82 nm. The idler blocker passed the band within 1505.55–1544.82 nm, that is, the idler light generated in the first lap was used as a transmit signal. The band of the transmit light through the 30.8-km PSCF was always 10.25 THz (1505.55–1587.25 nm) including idler light. We set the total input power to −5 dBm for the OPA. Therefore, the averaged fiber-input power was −6 dBm/ch. At the receiver side, the CUT was amplified with a rare earth-doped fiber amplifier in accordance with its wavelength. EDFAs were used for the C- and L-bands, and a thulium-doped fiber amplifier (TDFA) was used for the S-band. The CUT was then detected by a polarization-diverse coherent receiver after it was extracted by a BPF. The received signal was digitized using analog-digital convertors at 200 samples/s with a 70-GHz bandwidth and demodulated offline using a pilot-aided adaptation algorithm. After frontend error correction with a fixed linear equalizer, the CD was compensated for by frequency domain equalization. Signal equalization was performed with a complex 8×2 adaptive equalizer [1]. The adaptive filter in offline DSP was pre-converged by the data-aided least-mean square (LMS) algorithm. Then, the data tracking of the adaptive filter was performed by a decision-directed LMS algorithm and pilot-aided LMS algorithm utilizing a pilot symbol periodically inserted into the data. We also demodulated the idler light generated in the final lap.

Fig. 10 shows the optical spectra at the input of the loop and the output of the fiber at each lap. In these spectra, the measurement signal was inserted at 1553.3 nm. By increasing the number of laps, the outside of the spectra was slightly raised due to the non-flat gain profile with temperature detuning. The maximum number of laps was set to three because there was no gain-flattening filter in the loop to maintain the flatness of the WDM signal. Fig. 11 shows the NGMI of all channels after 92.4-km transmission. The NGMI of all 41 channels in each optical band was better than the threshold of 0.857. The NGMI dependence on wavelength was caused by the gain and NF characteristics of the optical amplifiers in the transmitter and receiver. The other

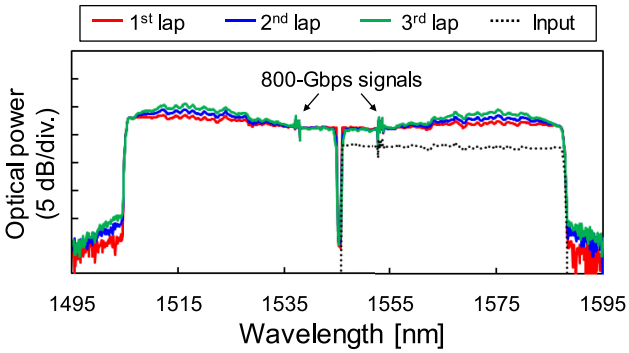

Fig. 10. Spectrum at output of PPLN-based OPA in each lap (0.1-nm resolution). 41-channel WDM signal was emulated by ASE light.

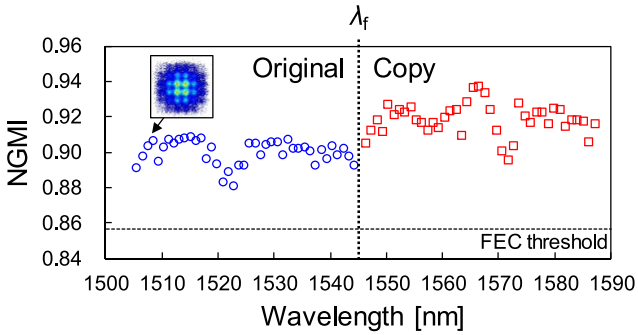

Fig. 11. NGMI results. Blue circular points indicate 41 transmitted original channels. Red square points indicate 41 channels copied in final lap.

reason was the wavelength dependence of components in the coherent receiver such as 90-degree hybrids and photodiodes. These results indicate that 5.125-THz inline-amplified transmission with our PPLN-based OPA can be achieved. In addition, by implementing the full-band configuration with an additional polarization-diverse OPA, the transmission bandwidth can be potentially extended to 10.25 THz across S-, C-, and L-bands well beyond the EDFA band. The small gain transient effect and wide-amplification bandwidth show that PPLN-based OPAs are promising as inline amplifiers for future optical transport networks that offer flexible utilization of abundant wavelength resources.

V. Simultaneous Inter-band Wavelength Conversion Using PPLN-based OPA

For multi-band WDM networks, we fabricated 4-port PPLN modules with a 1527.99-nm center wavelength for the QPM which is on the border between the C- and S-bands. We demonstrate inter-band wavelength conversion using the OPA with these modules. The simultaneous conversion of the transmission band is useful for constructing a multi-band optical network utilizing conventional C-band components [22], [40].

Fig. 12 shows the power saturation characteristic of the 4-port PPLN module. The input was CW light at 1545 nm. The gain of the PPLN module and input SH pump power were set to 16 dB and 1.1 W, respectively. The linear line indicates the in-out performance without gain saturation. The saturation output power with a gain reduction of 0.5 dB was 24.9 dBm.

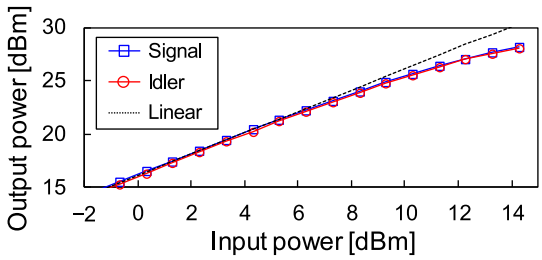

Fig. 12. Measurement of output power saturation of 4-port PPLN module for wavelength conversion between C- and S-bands. Input was single-polarized CW light at 1545 nm. Gain and SH pump power were 16.1 dB and 1 W, respectively.

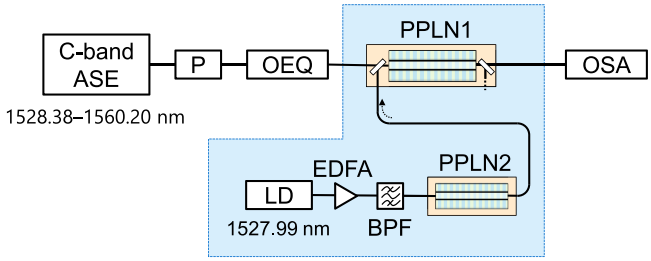

Fig. 13. Experimental setup for validation of simultaneous wavelength conversion between C- and S-bands. P: polarizer, OEQ: optical equalizer, LD: laser diode, BPF: band-pass filter, OSA: optical spectrum analyzer.

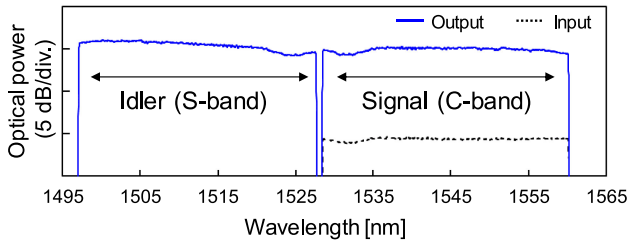

Fig. 14. Input and output spectra of our 4-port PPLN module with 1527.99-nm center wavelength for QPM (0.1-nm resolution). Input was 4-THz ASE light (1528.38–1560.20 nm).

No characteristic difference was observed between the signal and idler light. Next, we show simultaneous transmission band conversion between the C- and S-bands by amplifying C-band ASE light. Fig. 13 shows the experimental setup. The input light to the OPA was single-polarized 4-THz C-band ASE light (1528.38–1560.20 nm) at an optical power of 5 dBm. Fig. 14 shows the spectrum amplified by the OPA. It was confirmed that the input ASE light was copied in the S-band (1497.09–1527.60 nm). Conversion efficiency flatness in the idler band was within ± 1 dB. This result demonstrated the function of our PPLN-based OPA as a simultaneous inter-band wavelength convertor between C- and S-bands.

We conducted an experiment on the conversion of a modulated signal using the parallel-type polarization-diverse configuration. Using our OPA, we converted the C-band signal to the S-band and then back to the C-band (C-S-C conversion). The C-S-C converted signal was measured 50 times while scrambling the polarization in order to show that our polarization-diverse configuration is polarization-independent. Fig. 15 shows the experimental setup. A CUT at 1545.73 nm in the C-band was

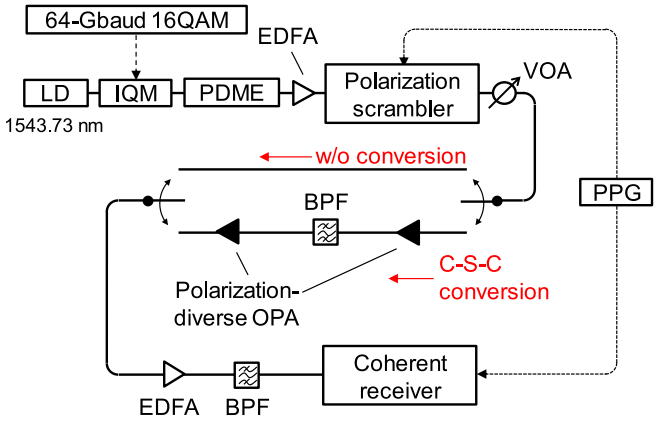

Fig. 15. Experimental setup for verification of wavelength conversion between S- and C-bands. LD: laser diode, IQM: I/Q modulator, PDME: polarization-division multiplexing emulator, VOA: variable optical attenuator, BPF: band-pass filter, PPG: pulse-pattern generator.

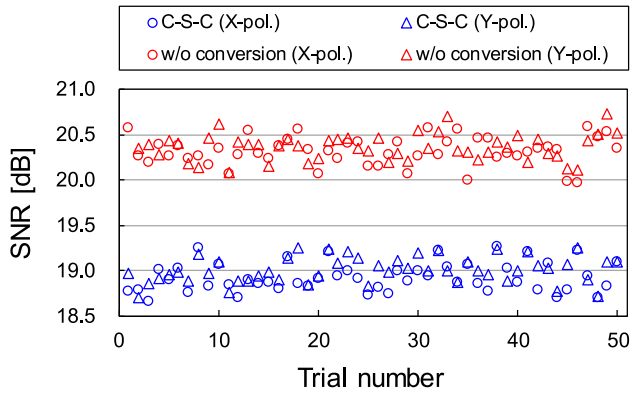

Fig. 16. Repeated test results of C-S-C conversion using our polarization-diverse PPLN-based OPA with 64-Gbaud DP-16QAM signal.

modulated with 64-Gbaud DP-16QAM and was input to a polarization scrambler after being amplified by a C-band EDFA. Then, the CUT was entered into the first polarization-diverse OPA and was converted to 1512.58 nm in the S-band as idler light. Only the idler component was extracted by a BPF and was entered into a second OPA. The CUT was returned to its original wavelength of 1545.73 nm and received by the coherent receiver via the C-band EDFA and the BPF. The input power of the CUT to each OPA was −5 dBm and −13 dBm, and the conversion efficiency of each OPA was −1.5 dB and 0 dB, respectively. The power of SH pump light input to each 4-port PPLN module was ∼200 mW, and the power of the pump light at 1527.99 nm input to PPLN for SHG was ∼500 mW. The polarization scrambler and the coherent receiver were synchronized by a trigger signal from a pulse pattern generator (PPG), and 50 measurements were performed while randomly modulating the polarization state of the CUT. The signal quality was evaluated by calculating the SNR after symbol decision. The results were compared with a no-conversion case. Fig. 16 shows the measurement results for each polarization component. In the no-conversion case, the standard deviations in SNR were 0.157 and 0.144 for each polarization. In the case with C-S-C conversion, the standard deviations of SNR were 0.158 and 0.142 for each polarization. If there were a gain difference between orthogonal polarization components and a PMD due to a delay mismatch in the polarization-diverse OPA, the fluctuation of the signal quality due to the polarization scramble should increase. This result indicates that our OPA was able to perform inter-band wavelength conversion without significant signal degradation due to impairment between polarization components.

VI. Conclusion

We reviewed recent research developments in the application of OPAs to wideband WDM transmission. OPAs have various functions, such as a wideband inline amplifier, wavelength converter, fiber-nonlinearity compensation, and phase-sensitive amplification, and their applications to multi-band WDM transmission is being studied. We introduced our research progress on WDM optical transmission using our PPLN-based OPA, that is, 10-THz-class inline amplification and simultaneous inter-band wavelength conversion. As reviewed above, the PPLN-based OPA has become applicable to practical optical communications through the progress of device technology that achieves both a wide-amplification bandwidth and high gain. It will be a key device for wideband and high-throughput WDM transmission in the future.

References

[1] T. Kobayashi *et al.*, "35-Tb/s C-band transmission over 800 km employing 1-Tb/s PS-64QAM signals enhanced by complex 8×2 MIMO equalizer," in *Proc. Opt. Fiber Commun. Conf.*, 2019, Paper Th4B.2.

[2] H. Masuda *et al.*, "20.4-Tb/s (204 × 111 Gb/s) transmission over 240 km using bandwidth-maximized hybrid Raman/EDFAs," in *Proc. Opt. Fiber Commun. Conf.*, 2007, Paper PDP20.

[3] M. Ionescu *et al.*, "74.38 Tb/s transmission over 6300 km single mode fiber with hybrid EDFA/Raman amplifiers," in *Proc. Opt. Fiber Commun. Conf.*, 2019, pp. 1–3.

[4] T. Kobayashi, A. Sano, A. Matsuura, Y. Miyamoto, and K. Ishihara, "Nonlinear tolerant spectrally-efficient transmission using PDM 64-QAM single carrier FDM with digital pilot-tone," *J. Lightw. Technol.*, vol. 30, no. 24, pp. 3805–3815, Dec. 2012.

[5] M. A. Iqbal, L. Krzczanowicz, I. Phillips, P. Harper, and W. Forysiak, "150 nm SCL-band transmission through 70 km SMF using ultra-wideband dual-stage discrete Raman amplifier," in *Proc. Opt. Fiber Commun. Conf.*, 2020, Paper W3E.4.

[6] F. Hamaoka *et al.*, "Ultra-wideband WDM transmission in S-, C-, and L-Bands using signal power optimization scheme," *J. Lightw. Technol.*, vol. 37, no. 8, pp. 1764–1771, Apr. 2019.

[7] J. Renaudier *et al.*, "First 100-nm continuous-band WDM transmission system with 115Tb/s transport over 100km using novel ultra-wideband semiconductor optical amplifiers," in *Proc. Eur. Conf. Opt. Commun.*, 2017, Paper Th.PDP.A.2.

[8] T. Kobayashi *et al.*, "Wide-band inline-amplified WDM transmission using PPLN-based optical parametric amplifier," *J. Lightw. Technol.*, vol. 39, no. 3, pp. 787–794, Feb. 2021.

[9] K. J. Lee *et al.*, "Phase sensitive amplification based on quadratic cascading in a periodically poled lithium niobate waveguide," *Opt. Exp.*, vol. 17, no. 22, pp. 20393–20400, Oct. 2009.

[10] B. J. Puttnam, D. Mazroa, S. Shinada, and N. Wada, "Phase-squeezing properties of non-degenerate PSAs using PPLN waveguides," *Opt. Exp.*, vol. 19, no. 26, pp. B131–B139, Nov. 2011.

[11] T. Kishimoto *et al.*, "Highly efficient phase-sensitive parametric gain in periodically poled $LiNbO_3$ ridge waveguide," *Opt. Lett.*, vol. 41, no. 9, pp. 1905–1908, May 2016.

[12] Y. M. Sua, J.-Y. Chen, and Y.-P. Huang, "Ultra-wideband and high-gain parametric amplification in telecom wavelengths with an optimally mode-matched PPLN waveguide," *Opt. Lett.*, vol. 43, no. 12, pp. 2965–2968, Jun. 2018.

[13] T. Kashiwazaki *et al.*, "Over-30-dB phase-sensitive amplification using a fiber-pigtailed PPLN waveguide module," in *Proc. Nonlinear Opt.*, 2019, Paper NW3A.2.

[14] P. A. Andrekson and M. Karlsson, "Fiber-based phase-sensitive optical amplifiers and their applications," *Adv. Opt. Photon.*, vol. 12, no. 2, pp. 367–428, Jun. 2020.

[15] T. Torounidis and P. A. Andrekson, "Broadband single-pumped fiber-optic parametric amplifiers," *IEEE Photon. Technol. Lett.*, vol. 19, no. 9, pp. 650–652, May 2007.

[16] R. Malik, A. Kumpera, M. Karlsson, and P. A. Andrekson, "Demonstration of ultra wideband phase-sensitive fiber optical parametric amplifier," *IEEE Photon. Technol. Lett.*, vol. 28, no. 2, pp. 175–177, 2015.

[17] T. Torounidis, P. A. Andrekson, and B.-E. Olsson, "Fiber-optical parametric amplifier with 70-dB gain," *Photon. Technol. Lett.*, vol. 18, no. 10, pp. 1194–1196, May 2006.

[18] G.-W. Lu, M. E. Marhic, and T. Miyazaki, "Burst-mode amplification of dynamic optical packets using fibre optical parametric amplifier in optical packet networks," *Electron. Lett.*, vol. 46, no. 11, pp. 778–780, 2010.

[19] C. B. Gaur *et al.*, "Comparison of erbium, Raman and parametric optical fiber amplifiers for burst traffic in extended PON," in *Proc. Opt. Fiber Commun. Conf.*, 2020, Paper W4B.3.

[20] Z. Ye *et al.*, "Overcoming the quantum limit of optical amplification in monolithic waveguides," *Sci. Adv.*, vol. 7, no. 38, pp. 1–6, Sep. 2021.

[21] J. Yamawaku *et al.*, "Low-crosstalk 103 channel × 10 Gb/s (1.03 Tb/s) wavelength conversion with a quasi-phase-matched $LiNbO_3$ waveguide," *J. Sel. Topics Quantum Electron.*, vol. 12, no. 4, pp. 521–528, Aug. 2006.

[22] T. Kato *et al.*, "Real-time transmission of 240×200-Gb/s signal in S+C+L triple-band WDM without S- or L-band transceivers," in *Proc. Eur. Conf. Opt. Commun.*, 2019, Paper PD.1.7.

[23] I. Sackey *et al.*, "Kerr nonlinearity mitigation: Mid-link spectral inversion versus digital backpropagation in 5×28-GBd PDM 16-QAM signal transmission," *J. Lightw. Technol.*, vol. 33, no. 9, pp. 1821–1827, May 2015.

[24] H. Hu *et al.*, "Fiber nonlinearity compensation by repeated phase conjugation in 2.048-Tbit/s WDM transmission of PDM 16-QAM channels," in *Proc. Opt. Fiber Commun. Conf.*, 2016, Paper Th4F.3.

[25] T. Umeki *et al.*, "Simultaneous nonlinearity mitigation in 92 × 180-Gbit/s PDM-16QAM transmission over 3840 km using PPLN-based guard-band-less optical phase conjugation," *Opt. Exp.*, vol. 24, no. 15, pp. 16945–16951, Jul. 2016.

[26] A. D. Ellis *et al.*, "4 Tb/s transmission reach enhancement using 10 × 400 Gb/s super-channels and polarization insensitive dual band optical phase conjugation," *J. Lightw. Technol.*, vol. 34. no. 8, pp. 1717–1723, Apr. 2016.

[27] K. Vijayan, B. Foo, M. Karlsson, and P. A. Andrekson, "Long-haul transmission of WDM signals with in-line phase-sensitive amplifiers," in *Proc. Eur. Conf. Opt. Commun.*, 2019, Paper P82.

[28] T. Umeki *et al.*, "Polarization-diversity in-line phase sensitive amplifier for simultaneous amplification of fiber-transmitted WDM PDM-16QAM signals," in *Proc. Opt. Fiber Commun. Conf.*, 2018, Paper M3E.4.

[29] S. Shimizu *et al.*, "8-Tbps (20 × 400 Gbps) unrepeated transmission over 80 km with 2-THz PPLN-based phase-sensitive amplification using precise chromatic dispersion pre-compensation," in *Proc. Eur. Conf. Opt. Commun.*, 2021, Paper Tu4C1.4.

[30] M. F. C. Stephens, M. Tan, V. Gordienko, P. Harper, and N. J. Doran, "In-line and cascaded DWDM transmission using a 15 dB net-gain polarization-insensitive fiber optical parametric amplifier," *Opt. Exp.*, vol. 25, no. 20, pp. 24312–24325, Oct. 2017.

[31] T. Kobayashi *et al.*, "13.4-Tb/s WDM transmission over 1,280 km repeated only with PPLN-based optical parametric inline amplifier," in *Proc. Eur. Conf. Opt. Commun.*, 2021, Paper Tu4C1.3.

[32] T. Torounidis, H. Sunnerud, P. O. Hedekvist, and P. A. Andrekson, "Amplification of WDM signals in fiber-based optical parametric amplifiers," *Photon. Technol. Lett.*, vol. 15, no. 8, pp. 1061–1063, Aug. 2003.

[33] J. B. Coles *et al.*, "Bandwidth-efficient phase modulation techniques for Stimulated Brillouin Scattering suppression in fiber optic parametric amplifiers," *Opt. Exp.*, vol. 18, no. 17, pp. 18138–18150, Aug. 2010.

[34] M. Jamshidifar, A. Vedadi, and M. E. Marhic, "Reduction of four-wave-mixing crosstalk in a short fiber-optical parametric amplifier," *Photon. Technol. Lett.*, vol. 21, no. 17, pp. 1244–1246, Sep. 2009.

[35] C. Langrock *et al.*, "All-optical signal processing using $\chi^{(2)}$ nonlinearities in guided-wave devices," *J. Lightw. Technol.*, vol. 24, no. 7, pp. 2579–2592, Jul. 2006.

[36] T. Umeki, O. Tadanaga, A. Takada, and M. Asobe, "Phase sensitive degenerate parametric amplification using directly-bonded PPLN ridge waveguides," *Opt. Exp.*, vol. 19, no. 7, pp. 6326–6332, Mar. 2010.

[37] T. Umeki, T. Kazama, H. Ono, Y. Miyamoto, and H. Takenouchi, "Spectrally efficient optical phase conjugation based on complementary spectral inversion for nonlinearity mitigation," in *Proc. Eur. Conf. Exhib. Opt. Commun.*, 2015, Paper We2.6.2.

[38] S. Yoshima *et al.*, "Nonlinearity mitigation through optical phase conjugation in a deployed fibre link with full bandwidth utilization," in *Proc. Eur. Conf. Opt. Commun.*, 2015, Paper We2.6.3.

[39] A. D. Ellis *et al.*, "Enhanced superchannel transmission using phase conjugation," in *Proc. Eur. Conf. Exhib. Opt. Commun.*, 2015, Paper We2.6.4.

[40] H. Kawahara, M. Nakagawa, T. Seki, and T. Miyamura, "Experimental demonstration of wavelength-selective band/direction-switchable multi-band OXC using an inter-band all-optical wavelength converter," in *Proc. Eur. Conf. Opt. Commun.*, 2020, Paper Tu1H-5.

[41] S. L. I. Olsson *et al.*, "Phase-sensitive amplified transmission links for improved sensitivity and nonlinearity tolerance," *J. Lightw. Technol.*, vol. 33, no. 3, pp. 710–721, Nov. 2015.

[42] K. Vijayan, B. Foo, M. Karlsson, and P. A. Andrekson, "Cross-phase modulation mitigation in phase-sensitive amplifier links," *IEEE Photon. Technol. Lett.*, vol. 31, no. 21, pp. 1733–1736, Sep. 2019.

[43] T. Kazama *et al.*, "Over-30-dB gain and 1-dB noise figure phase-sensitive amplification using pump-combiner-integrated fiber I/O PPLN module," *Opt. Exp.*, vol. 29, no. 18, pp. 28824–28834, Aug. 2021.

[44] S. L. I. Olsson *et al.*, "Injection locking-based pump recovery for phase-sensitive amplified links," *Opt. Exp.*, vol. 21, no. 12, pp. 14512–14529, Jun. 2013.

[45] Y. Okamura *et al.*, "Optical pump phase locking to a carrier wave extracted from phase-conjugated twin waves for phase-sensitive optical amplifier repeaters," *Opt. Exp.*, vol. 24, no. 23, pp. 26300–26306, Nov. 2016.

[46] S. L. I. Olsson, H. Eliasson, E. Astra, M. Karlsson, and P. A. Andrekson, "Long-haul optical transmission link using low-noise phase-sensitive amplifiers," *Nat. Commun.*, vol. 9, Jun. 2018, Paper 2513.

[47] S. Shimizu *et al.*, "Accurate estimation of chromatic dispersion for non-degenerate phase-sensitive amplification," *J. Lightw. Technol.*, vol. 39, no. 1, pp. 24–32, Jan. 2021.

[48] T. Kazama *et al.*, "Low-parametric-crosstalk phase-sensitive amplifier for guard-band-less DWDM signal using PPLN waveguides," *J. Lightw. Technol.*, vol. 35, no. 4, pp. 755–761, Aug. 2016.

[49] K. K. Y. Wong, M. E. Marhic, K. Uesaka, and L. G. Kazovsky, "Polarization-independent one-pump fiber-optical parametric amplifier," *Photon. Technol. Lett.*, vol. 14, no. 11, pp. 1506–1508, Nov. 2002.

[50] M. Jazayerifar *et al.*, "Impact of SBS on polarization-insensitive single pump optical parametric amplifiers based on a diversity loop scheme," in *Proc. Eur. Conf. Opt. Commun.*, 2014, Paper Tu.4.6.4.

[51] V. Gordienko, F. M. Ferreira, C. B. Gaur, and N. J. Doran, "Looped polarization-insensitive fiber optical parametric amplifiers for broadband high gain applications," *J. Lightw. Technol.*, vol. 39, no. 19, pp. 6045–6053, Oct. 2021.

[52] F. Bessin, V. Gordienko, F. M. Ferreira, and N. Doran, "First experimental Mach-Zehnder FOPA for polarization- and wavelength-division-multiplexed signals," in *Proc. Eur. Conf. Opt. Commun.*, 2021, Paper Tu2A.6.

[53] T. Umeki *et al.*, "PDM signal amplification using PPLN-based polarization-independent phase-sensitive amplifier," *J. Lightw. Technol.*, vol. 33, no. 7, pp. 1326–1332, Apr. 2015.

[54] M. Asobe, T. Umeki, and O. Tadanaga, "Phase sensitive amplification with noise figure below the 3 dB quantum limit using CW pumped PPLN waveguide," *Opt. Exp.*, vol. 20, no. 12, pp. 13164–13172, May 2012.

[55] D. J. Elson *et al.*, "Investigation of bandwidth loading in optical fibre transmission using amplified spontaneous emission noise," *Opt. Exp.*, vol. 25, no. 16, pp. 19529–19537, Aug. 2017.

[56] F. Hamaoka *et al.*, "120-GBaud 32QAM signal generation using ultra-broadband electrical bandwidth doubler," in *Proc. Opt. Fiber Commun. Conf.*, 2019, Paper M2H.6.

[57] M. Nakamura *et al.*, "Entropy and symbol-rate optimized 120 GBaud PS-36QAM signal transmission over 2400 km at net-rate of 800 Gbps/λ," in *Proc. Opt. Fiber Commun. Conf.*, 2020, Paper M4K.3.

[58] A. Matsushita *et al.*, "64-GBd PDM-256QAM and 92-GBd PDM-64QAM signal generation using precise-digital-calibration aided by optical-equalization," in *Proc. Opt. Fiber Commun. Conf.*, 2019, Paper W4B.2.

Shimpei Shimizu (Member, IEEE) received the B.E. degree in engineering and the M.E. degree in information science and technology in the field of electronics for informatics from Hokkaido University, Sapporo, Japan, in 2016 and 2018, respectively. In 2018, he joined the NTT Network Innovation Laboratories, Yokosuka, Japan. His current research focuses on high-capacity optical transmission systems. He is a Member of the Institute of Electronics, Information and Communication Engineers (IEICE) of Japan and the IEEE Photonics Society. He was the recipient of the 2017 IEICE Communications Society Optical Communication Systems Young Researchers Award.

Takayuki Kobayashi (Member, IEEE) received the B.E., M.E., and Dr. Eng. degrees from Waseda University, Tokyo, Japan, in 2004, 2006, and 2019, respectively. In April 2006, he joined the NTT Network Innovation Laboratories, Yokosuka, Japan, where he was engaged in the research on high-speed and high-capacity digital coherent transmission systems. In April 2014, he moved to the NTT Access Network Service Systems Laboratories, Yokosuka, and was engaged in 5G mobile optical network systems. In July 2016, he moved back to the NTT Network Innovation Laboratories and has been working on high-capacity optical transmission systems. His current research interests include long-haul optical transmission systems employing spectrally efficient modulation formats enhanced by digital and optical signal processing. He is a Member of the Institute of Electronics, Information and Communication Engineers (IEICE) of Japan. From 2016 to 2018, he was a Technical Program Committee (TPC) Member of the Electrical Subsystems' Category for the Optical Fiber Communication Conference (OFC). Since 2018, he has been a TPC Member of the Point-to-Point Optical Transmission Category for the European Conference on Optical Communication (ECOC).

Takushi Kazama received the B.S. and M.S. degrees in electrical engineering from The University of Tokyo, Tokyo, Japan, in 2009 and 2011, respectively. In 2011, he joined the NTT Device Technology Laboratories, Japan, where he is engaged in research on nonlinear optical devices based on periodically poled $LiNbO_3$ waveguides. He is a Member of the Institute of Electronics, Information, and Communication Engineers of Japan (IEICE) and the Japan Society of Applied Physics (JSAP).

Takeshi Umeki (Member, IEEE) received the B.S. degree in physics from Gakusyuin University, Tokyo, Japan, in 2002, and the M.S. degree in physics and the Ph.D. degree in nonlinear optics from The University of Tokyo, Tokyo, Japan, in 2004 and 2014, respectively. In 2004, he joined the NTT Photonics Laboratories, Atsugi, Japan, since then, he has been involved in research on nonlinear optical devices based on periodically poled $LiNbO_3$ waveguides. He is a Member of the Japan Society of Applied Physics (JSAP), the Institute of Electronics, Information, and Communication Engineers (IEICE), and the IEEE/Photonics Society.

Masanori Nakamura (Member, IEEE) received the B.S. and M.S. degrees in applied physics from Waseda University, Tokyo, Japan, in 2011 and 2013, respectively, and the Ph.D. degrees in electrical, electronic, and infocommunications engineering from Osaka University, Osaka, Japan, in 2021. In 2013, he joined NTT Network Innovation Laboratories, Yokosuka, Japan, where he engaged in research on high-capacity optical transport networks. He is a Member of the Institute of Electronics, Information, and Communication Engineers, Tokyo, Japan. He was the recipient of the 2016 IEICE Communications Society Optical Communication Systems Young Researchers Award.

Koji Enbutsu received the B.E. and M.E. degrees in electronics engineering from Hokkaido University, Sapporo, Japan, in 1994 and 1996, respectively. In 1996, he joined the NTT Opto-Electronics Laboratories, Japan, where he engaged in research on organic optical waveguides for optical communications and electro-optic crystals and their devices. In 2007, he moved to the NTT Access Services Network System Laboratories, where he engaged in research on optical fiber testing and monitoring. He is a Member of the Institute of Electronics, Information, and Communication Engineers (IEICE) and Japan Society of Applied Physics (JSAP).

Takahiro Kashiwazaki received the B.E. and M.E. degrees in materials science from Keio University, Tokyo, Japan, in 2013 and 2015, respectively. In 2015, he joined the NTT Device Technology Laboratories, Atsugi, Japan. He is conducting research on periodically poled lithium niobate waveguide devices. He is a Member of the Institute of Electronics, Information, and Communication Engineers of Japan (IEICE) and Japan Society of Applied Physics (JSAP).

Ryoichi Kasahara received the B.S. degree from The University of Electro-Communications, Tokyo, Japan, in 1995, and the M.S. degree from Tohoku University, Sendai, Japan, in 1997. In 1997, he joined the NTT Opto-Electronics Laboratories, Japan, where he was involved in research on silica-based planar lightwave circuits (PLCs), including thermo-optic switches and arrayed-waveguide grating multiplexers, and integrated optoelectrical receiver modules. He is currently with the NTT Device Technology Laboratories, Japan, where he is involved in the research and development of the fabrication technologies of optical dielectric waveguide devices. He is a Senior Member of the Institute of Electronics, Information, and Communication Engineers of Japan (IEICE) and a Member of the Japan Society of Applied Physics (JSAP).

Kei Watanabe received the B.E., M.E., and Dr. Eng. degrees in physical electronics from Kobe University, Kobe, Japan, in 1998, 2000, and 2003, respectively. In 2004, he joined NTT Laboratories, Kanagawa, Japan, where he engaged in research on silica-based optical waveguides. From 2008 to 2009, he was a Visiting Researcher with Photonic Research Group, Ghent University, Ghent, Belgium, where he focused on uniting silicon photonics and silica-based optical waveguides. Since 2009, he has been engaged in the development of InP-based high-speed Mach–Zehnder modulators. He is a Member of the Japan Society of Applied Physics, the Institute of Electronics, Information, and Communication Engineers of Japan, and IEEE Photonics Society.

Yutaka Miyamoto (Member, IEEE) received the B.E. and M.E. degrees in electrical engineering from Waseda University, Tokyo, Japan, in 1986 and 1988, respectively, and the Dr. Eng. degree in electrical engineering from Tokyo University, Tokyo, in 2016. In 1988, he joined NTT Transmission Systems Laboratories, Yokosuka, Japan, where he was engaged in the research and development of highspeed optical communications systems including the 10-Gbit/s first terrestrial optical transmission system (FA-10G) using erbium-doped fiber amplifiers (EDFA) inline repeaters. From 1995 to 1997, he was with NTT Electronics Technology Corporation, Yokohama, Japan, where he was engaged in the planning and product development of high-speed optical module at the data rate of 10 Gb/s and beyond. Since 1997, he has been with NTT Network Innovation Laboratories, Yokosuka, where he has contributed to the research and development of optical transport technologies based on 40/100/400-Gbit/s channel and beyond. He is currently a NTT Fellow and the Director of the Innovative Photonic Network Research Center, NTT Network Innovation Laboratories, where he is investigating and promoting the future scalable optical transport network with the Pbit/s-class capacity based on innovative transport technologies such as digital signal processing, space division multiplexing, and cutting-edge integrated devices for photonic preprocessing. He is a Fellow of the Institute of Electronics, Information, and Communication Engineers (IEICE).